Materials Research Proceedings 41 (2024) 2329-2338 https://doi.org/10.21741/9781644903131-256

Accurate 3D modeling of laser-matter interaction in the AFP process by a conductive-radiative FEM approach

STORTI Bruno A.[1,a*], LE REUN Adrien[1,b], LE CORRE Steven[1,c]

[1] Nantes Université, CNRS, LTEN, UMR 6607, La Chantrerie, Rue Christian Pauc, Nantes, 44200, Pays de la Loire, France

[a]bruno.storti@univ-nantes.fr, [b]adrien.le-reun@univ-nantes.fr, [c]steven.lecorre@univ-nantes.fr

Keywords: AFP, Conductive-Radiative Heat Transfer, Finite Elements

Abstract. Mainly driven by aeronautical demands, the Automated Fiber Placement (AFP) process has become pivotal in the in-situ manufacturing of intricate, high-performance composite components. AFP relies on robotic systems to meticulously lay continuous fiber-reinforced materials, employing controlled pressure and precise laser heating. Accurate thermal modeling is imperative to predict thermal effects impacting contact, adhesion, crystallinity, and residual constraints. This work introduces a novel numerical approach for efficient modeling the transient heat transfers in the AFP process using a coupled conductive-radiative finite element method (FEM) scheme. Radiative density from the laser-matter interaction is determined through an in-house parallelized FreeFEM++ code. Heat transfer at the micro-scale is assessed by using an artificial computational geometry based on fiber distributions obtained from tape micrograph. A parametric study with varying absorption coefficients of the carbon fibers is performed to accurately compute the radiative volumetric heat source. The proposed approach investigates various 2D and 3D scenarios involving different laser parameters. Results exhibit strong agreement with experimentally obtained data, showing a maximum temperature difference of 5-6°C at the end of the heating phase. Furthermore, a 3D case demonstrates the potential of this approach for modeling complex micro-scale geometries.

Introduction

The Automated Fiber Placement (AFP) is an established manufacturing process to efficiently produce large and complex high-performance composite parts featuring high strength-to-weight ratios, a characteristic which is highly demanded by the aeronautic industry, among others. The AFP is a layer-by-layer in-situ manufacturing technique which mainly consists in rapidly heating both the new layer of the tape and the substrate composite materials with a laser source to reach temperatures above the thermoplastic matrix melting point. This heating stage is followed by a rapid cooling stage where a controlled pressure is applied between the already deposed tape and the substrate to achieve a proper material consolidation.

Among the multiple physics involved during such a complex manufacturing procedure, the numerical modelling of the heat transfer is the most crucial and challenging one, since an accurate prediction of the thermal history is necessary for the proper modelling of factors such as intimate contact, autohesion, residual stress, and crystallinity during consolidation [1,2]. Several numerical approaches have been proposed in the literature for heat transfer modelling in the AFP context. For instance, in the work of [3] a surface-to-surface heat transfer radiation model was developed in Matlab for 3D surfaces where the laser diode and tape were discretized in a finite number of differential areas, and the energy exchanged was computed depending on their sizes, separation distance, and orientation angle. Consequently, the computed heat flux is applied as a boundary condition at the tape surface in a 2D transient heat conduction model. In the thesis work of [4], a comprehensive 2D transient heat conduction model was developed in COMSOL accounting for the roller, the laying tape, the substrate, and the tool, while the laser beam was modeled by a heat

flux boundary condition obtained via a ray-tracing (RT) approach. In [5] a Matlab RT implementation was coupled to a 2D transient thermal model developed in ABAQUS for tape consolidation studies in the AFP process. The heat flux distributions in the tape and substrate were characterized in terms of the laser incidence angle, wavelength, head tilt, and the contact width of the roller. Subsequently, a heat flux boundary condition was imposed in the thermal model at both the surfaces of the incoming tape and substrate obtained from RT.

A shared characteristic among the aforementioned methodologies is their exclusive reliance on angular decomposition between the laser beam and idealized smooth substrate/tape surfaces to estimate heat flux, neglecting the composite's micro-structure and/or surface irregularities. Recent investigations [6,7,8] highlight the importance of accounting for the micro-structural topology of fibers within the thermoplastic matrix when modeling laser-matter interactions. This emphasis is driven by the notable contrast in thermal properties within the composite, where the laser predominantly penetrates the semi-transparent thermoplastic matrix with minimal interaction, and which is primarily absorbed/reflected by the fibers. In [8], the fibers' geometry is depicted as a structured array of evenly spaced 10μm half cylinders across the composite surface, utilizing the RT method to analyze the composite's scattering behavior. A notable advancement in micro-structure thermo-optical modeling is detailed in [6,7], where authors utilized an artificially generated representative geometry. Employing the RT approach, they identified the laser impact zone on fiber surfaces and enforced a heat flux boundary condition on these surfaces. A significant finding from [6] indicates that precise determination of radiative volumetric heat sources may notably improve temperature prediction accuracy when employing homogenized composite structures in comparison with a standard surface heat flux condition.

In this work a novel numerical approach for thermal modelling at the micro-scale of a composite tape during AFP manufacturing conditions is proposed. The scheme is based on employing an efficient RTE solver developed in FreeFEM++ [9] as part of the thesis work of [10,11] to obtain the radiative heat source within the composite, and then coupling the solution to transient 2D and 3D heat conduction simulations. The RTE-FEM solver is based on the Discrete Ordinates Method (DOM) where an angular discretization is required in addition to the spatial FEM mesh. Being an accurate although memory demanding approach, the solution is obtained in parallel by using the PETSc libraries on a High-Performance Computer cluster.

Study Case at the Composite Micro-scale

The radiative-conductive coupling scheme is to be applied at the micro-scale of a single tape which is considered to be stationary. To be able to compare the radiative-conductive solution with respect to both a numerical thermo-optical model and experimental results, the micro-structure of the tape analyzed here is identically to the one presented [7], where the composite material is made of a matrix of the high-performance polymer PEKK7002 reinforced with carbon fiber of the AS7 type. A micrograph of the composite micro-structure is depicted Fig. 1a. A comprehensive imaging analysis was developed in [6,7] to accurately represent the real micro-structure by an artificial computational one (see Fig. 1b) which is able to reproduce the fiber volume fraction (FVF) in the thickness of the composite tape. Hence, the geometry depicted in Fig. 1b is employed throughout this work. We refer the readers to the previously mentioned article for more insights regarding the micro-structure generation procedure.

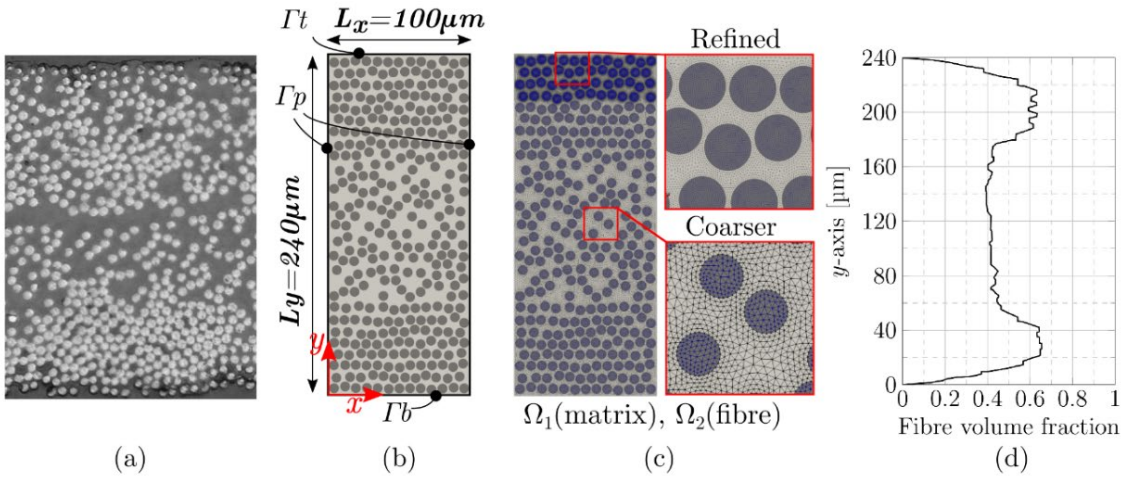

Figure 1: Micro-structure of the composite tape taken from [7]: (a) optical micrograph, (b) micro-structure generated artificially, (c) FEM mesh, (d) the distribution of the FVF.

The representative geometry of the tape is 100μm width and 240μm height, and the fibers are 6.9μm diameter. The average FVF is 50%, where, as observed in Fig. 1d, the distribution is denser near the surfaces, achieving roughly 60%, and less dense in the center, where the FVF reduces to 40%. This is particularly important since, as will be developed later, the intensity of the laser is mostly absorbed by the first's fiber layers of the tape. In addition, Fig. 1c showcases the unstructured mesh of the micro-structure to be used by the FEM solvers, and which will be further explained in the following sections.

Governing Equations and Numerical Model

The numerical modelling of the laser-matter interaction during the AFP process is developed in two stages throughout this work: first, the modelling of the radiative heat transfer between the laser beam and the composite micro-structure, and second, the modelling of the transient conductive heat transfer within the matrix and the fibers. Next, the governing equations are addressed.

The Discrete Ordinates Model (DOM) in Radiative Heat Transfer. The RTE is that of the monochromatic steady state defined as follows:

$$\big(s\cdot\nabla+\beta(x)\big)I_\lambda(x,s)=\frac{\sigma_s}{4\pi}\oint_{s'=4\pi}I_\lambda(x,s')\Phi(s,s')ds'+\kappa(x)I_b(T,\lambda)\quad\forall\mathbf{x}\in\Omega,s\in S, \tag{1}$$

where $\mathbf{x}=(x,y,z)$ and $s=(\phi,\theta)$ are the spatial and direction vectors, respectively, I_λ is the radiative intensity at a given wavelength λ, κ and σ_s the absorption and scattering coefficients, Φ the scattering phase function, which defines the probability of a photon traveling in the $\boldsymbol{s}$ direction to be redirected to some other direction $\boldsymbol{s}'$, and $\beta=(\sigma_s+\kappa)$ stands for the extinction coefficient. To solve the RTE, a FEM formulation is employed here by employing a parallelized code developed in FreeFEM++[10] and compiled with PETSc. The FEM-RTE model is based on the DOM for radiation which solves the RTE for a finite number of discrete solid angles. Thus, after the discretization of the angular space S by a set of N_d discrete directions $(s_1,s_2,\dots,s^{N_d})\in S^{N_d}$ the equation of the RTE yields:

$$\big(\boldsymbol{s}_m\cdot\nabla+\beta(x)\big)I_{m\lambda}(x,s)=\sigma_s\sum_{n=1}^{N_d}\omega_nI_{n\lambda}(x)\Phi_{m,n}+\kappa(x)I_b(T,\lambda)\quad\forall m=1,\dots,\mathrm{N_d} \tag{2}$$

where $\boldsymbol{s}_m$ represents the discrete directions vector obtained by the successive discretization of an unit circle, for a 2D case, or a unit sphere, for a 3D one, and ω_n is the quadrature weight. Following previous works of radiation in heterogeneous materials with inclusions and high contrast radiative properties [10], the in-scattering effects are modeled using the Henyey-Greenstein phase function Φ [10], with an anisotropic coefficient g = 0.8. Following the angular discretization, a standard

space discretization with unstructured triangles/tetrahedral elements is performed and a vectorized FEM formulation is employed in this work [10,11]. Due to the advective-dominant nature of the RTE, the FEM equations are stabilized by the Streamlined-Upwind Petrov-Galerkin (SUPG) stabilization term [10,12].

Boundary Conditions in the RTE. To model the laser radiation applied to the top surface of the composite tape Γ_t (see Fig. 1b), the following collimated boundary condition is considered:

$$I_{collimated} = I_w(x_w, s) = \begin{cases} I_0\,, & \forall x_w \in \Gamma_t \quad \text{if } s = s_c, \\ 0\,, & \forall x_w \in \Gamma_t \quad \text{if } s \neq s_c, \end{cases} \tag{3}$$

where I_0 is the radiative intensity strength of the diode laser beam. Following the experimental works reported in [7], two boundary conditions are considered for the laser beam: a near-normal incidence angle $\theta = 15°$ with $I_0 = 1.47\text{Wmm}^{-2}$, and a grazing incidence angle with $\theta = 60°$ and $I_0 = 2.793\text{Wmm}^{-2}$. Moreover, Γ_p is treated as periodic.

Transient Conductive-Radiative Heat Transfer Equation. The transient heat transfer

Form including the radiation and conduction yields:

$$\rho Cp\left(\frac{\partial T(t,\mathbf{x})}{\partial t}\right) = -\nabla \cdot \left(Q_r(T,\lambda,\mathbf{x}) + Q_c(t,\mathbf{x})\right) \quad \forall \mathbf{x} \in \Omega, \forall t > 0, \tag{4}$$

where ρ and Cp stand for the material density and specific heat capacity, respectively, and $\nabla \cdot Q_r(T,\lambda,\mathbf{x})$ and $\nabla \cdot Q_c(t,\mathbf{x})$ are the radiative and conductive volumetric sources, respectively. The later is defined from the Fourier's law as $\nabla \cdot Q_c(t,\mathbf{x}) = -k\nabla T(t,\mathbf{x})$, being k the thermal conductivity of the material, and the radiative source term is as:

$$\nabla \cdot Q_r(T,\lambda,\mathbf{x}) = \kappa 4\pi I_b(T,\lambda) - \kappa G(\mathbf{x}), \tag{5}$$

where $G(\mathbf{x})$ is the radiative density obtained by the RTE solver, which is computed at a given point $\mathbf{x}$ in a participating medium as $G(x) \approx \sum_{n=1}^{N_d} I_n(x)\omega_n$, and I_b stands for the black body source term. For the present study case where temperatures are expected to reach ≈ 200°C, the I_b term can be neglected, since it results of orders of magnitude lower than that of $\kappa G(\boldsymbol{x})$. In this way, the radiative and conductive heat transfer equations can be weakly coupled, i.e., the RTE is solved once for a given incidence angle and intensity of the laser, and its solution is coupled to the transient conductive equation via the volumetric source term.

Parametric Analysis and RTE vs. RT Comparison

Parametric Study of Varying Absorption Coefficients. To characterize the properties of the matrix (Ω_1) and fiber (Ω_2) materials, proper values of the σ_s and κ coefficients must be used in the RTE solver. Given their unavailability, a parametric study has been conducted. Its purpose is to ascertain a more fitting collection of parameters that effectively characterize the laser-matter interaction. The composite sample can be modeled as a combination of a highly absorbing medium for the carbon fibers, and a semi-transparent one for the polymer matrix [10]. Then, the adopted parameters to perform the parametric study are depicted in Table 1, being κ_2 recognized as the most relevant one.

Table 1: Boundary conditions and thermal properties used for the radiative parametric study. I_0 is given in [Wmm^{-2}], θ in [°], and σ_s and κ in [mm^{-1}].

	I_0	θ	σ_{s1}	σ_{s2}	κ_1	κ_2
Near-normal incidence	1.47	15	0.01	0.01	0.01	200,400,600,800,1000
Grazing incidence	2.793	60	0.01	0.01	0.01	200,400,600,800,1000

Furthermore, the radiative volumetric source $\nabla \cdot Q_r(y)$ is computed by Eqn. (5) along the tape y-axis from the FEM solution as follows:

$$\nabla \cdot Q_r(y) = \frac{1}{\Delta y}\int_{y-\Delta y/2}^{y+\Delta y/2} \kappa(x)G(x)dy \approx \frac{1}{\Delta y}\left(\sum_{i=1}^{2}\sum_{j=1}^{n_e} \kappa_i G_i\left(e^j\right)A^j\right) , \quad (6)$$

where $G_i\left(e^j\right)$ corresponds to the radiative density solution at the element e^j of the Ω_i domain, A_j stands for the element area/volume, Δy are discretized thicknesses of 0.2µm, and n_e the number of elements located at such thickness.

For solving the RTE the mesh shown in Fig. 1c was employed with 147.475 non-structured triangular elements refined towards the top surface of the domain. A total of $N_d = 80$ directions was employed for the angular discretization. Each simulation took roughly 4 minutes solving with GMRES and running in 80 cores of the cluster CCIPL located at *Le centre de calcul intensif des Pays de la Loire*, in France. The results of the radiative volumetric source for the near-normal incidence case obtained at 20µm thickness of the composite is observed in Fig. 2a. It is to notice that for $\kappa_2 = 200\text{mm}^{-1}$, the radiative density increases into the thickness of the composite tape, achieving a maximum peak at a roughly 3.75µm from the surface. As κ_2 increases, the maximum peak is given closer to the tape surface at thickness of roughly 2.5µm. This become evident from the RTE solution for three reprensentative cases in Fig. 2b, where it is shown that as κ_2 increases, the radiative density is further concentrated at the top surface of the first layers of the carbon fibers. Furthermore, it is worth noticing that the main peak of the volumetric heat source increases of approximately 87% when κ_2 increases from 200mm^{-1} to 600mm^{-1}. This is of importance since, as will be shown later, a proper representation of such a term will impact in the accuracy at the moment of predicting the tape surface temperature during the AFP process.

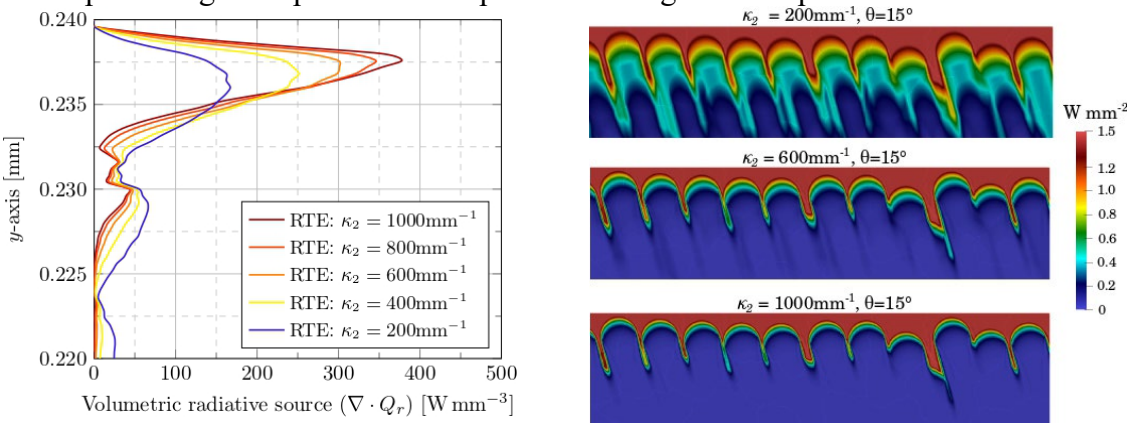

(a) (b)

Figure 2: Parametric results of the RTE for the near-normal incidence case: (a) the heat source distribution at the near surface of the composite, and (b) the radiative density field.

In Fig. 3 are presented the results obtained from the RTE solver for the grazing laser beam case. Similar conclusions can be obtained as compared to the results obtained for $\theta = 15°$. Nevertheless, it should be noticed that for $\theta = 60°$ the distribution of the volumetric heat source is further concentrated at the surface of the tape, where the laser energy is almost totally absorbed at the 10µm thickness for $\kappa_2 > 200\text{mm}^{-1}$ (see Fig. 3a).

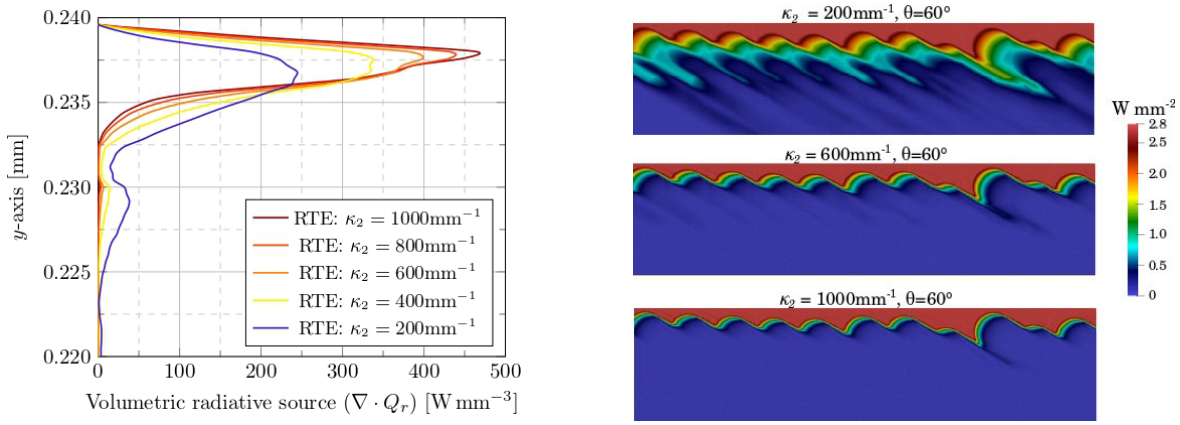

(a) (b)

Figure 3: Parametric results of the RTE for the grazing incidence case: (a) the heat source distribution at the near surface of the composite, and (b) the radiative density field.

RTE vs RT Comparison. As a part of a previous work [6] the volumetric heat source distribution was obtained by the RT approach using a home-made Matlab code which considered the matrix as a full transparent material, and where the laser absorption is only given at the fiber surfaces by a purely geometrical approach. In Fig. 4 are compared the solutions obtained by the RTE with respect to that of RT, and to a double-beta fit function [6]. When using $\kappa_2 = 600\text{mm}^{-1}$, a well-matched volumetric heat source distribution is observed for a near-normal incidence (see Fig. 4a), resembling the double-beta function, accurately reproducing the closest-to-surface peak. Additionally, under grazing laser incidence (see Fig. 4b), the RTE solution replicates the volumetric heat source feature noted in [6], displaying a single dominant peak.

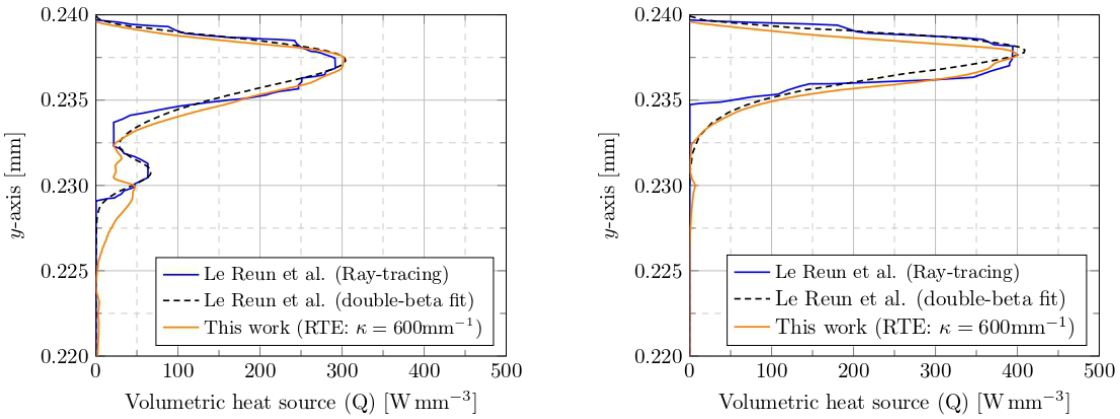

(a) (b)

Figure 4: Radiative source distribution across a 20μm composite depth alongside a comparative assessment against a previously published RT-based approach.

Results of RTE-Conductive Coupling on Composite Micro-structure

Experimental Setup Description. The thermophysical properties of the composite material to be used by the radiative-conductive coupling are the same as those reported in [6] and are recalled here in Table 2. The experimental reproduction of the AFP process and the temperature measurements were performed on an ad-hoc bench, which possess a rotating 2kW laser diode of the type LDM 200-6000 with adjusting incidence angle and distance to the tape surface. The laser diode was set to irradiate the composite at λ = 980nm with controlled time and power. The temperature at the tape surface was measured by an infrared camera FLIR XC609. We refer the readers to the Refs. [6, 7] for further details regarding the experimental setup. For the transient

heat transfer problem, the heating time of the laser is set to $t_c = 20$ms, which corresponds to the exposure time in an AFP manufacturing process where the laying speed is 500ms with a 12mm laser beam width. The experience lasted a total of $t_t = 40$ms.

Table 2: Thermal properties of the matrix and the carbon fibers. k is given in [$Wm^{-1}K^{-1}$], ρ in [$kg\ m^{-3}$], C_p in [$Jkg^{-1}K^{-1}$], and σ_s and κ in [mm^{-1}].

	k	ρ	Cp	σ_s	κ
PEKK7002	0.27	1290	$T \leq T_g, 3.35T[°C] + 1017.0$ $T_g < T < T_m, 3.45T[°C] + 1137.6$	0.01	0.01
Carbon fibre AS7	2.2	1790	$-0.00295T[°C]^2 + 3.493T[°C] + 578$	0.01	600

Radiative-Conductive Coupling Algorithm and 2D Case Results. The Algorithm 1 is used to solve the radiative-conductive equations in the artificially generated composite micro-structure under AFP conditions, where δ_t is the time-step discretization employed by the Crank-Nicolson scheme ($\delta_t = 0.5$s), and $\{X_c, d\}$ are the fiber coordinates and diameter, respectively. The boundary conditions for the coupled radiative-conductive problem are: a third type boundary condition at the top composite surface Γ_t (see Fig. 1b) defined as $-k(\partial T/\partial n) = h_c(T - T_{amb})$, being n the outward normal vector, T_{amb} the ambient temperature considered at 20°C, and h_c a convective exchange coefficient with the surrounding air of 5$Wm^{-2}K^{-1}$; isolated boundaries at Γ_p modeled as $-k(\partial T/\partial n) = 0$; and a perfect contact at the composite-tool interface Γ_b, with an imposed temperature of $T = T_{tool}$, considering the tool to be at T_{amb}.

Algorithm 1: RTE-conduction of AFP process on composite microstructure

Input : $\{X_c, d\}$, $\{I, \theta\}$, $\{t_t, t_c, \delta t\}$, $\{\rho, k, Cp, \kappa, \sigma\}_{1,2}$, $\{h_c, T_{amb}, T_{tool}\}$
Define: T_N, T_{N+1}, T_i

$\Omega_1^h \cup \Omega_2^h \leftarrow$ Generation of artificial micro-structure from $\{X_c, d\}$, and meshing;
$G(\mathbf{x}) \leftarrow$ **solve** the RTE on $\Omega_1^h \cup \Omega_2^h$ with $\{I, \theta\}$, and $\{\kappa_1, \sigma_1, \kappa_2, \sigma_2\}$;
$\nabla \cdot Q_r \leftarrow$ compute radiative heat source term with $G(\mathbf{x})$ and $\{\kappa_1, \kappa_2\}$;
$T_N = T_i$
for $t < t_t$: $t = t + \delta t$; **do**
  if $t \leq t_c$ **then**
    $T_{N+1} \leftarrow$ **solve** conduction eq. using $\nabla \cdot Q_r, T_N, \{\rho, k, C_p\}_{1,2}$, and $\{h_c, T_{amb}, T_{tool}\}$
  else
    $T_{N+1} \leftarrow$ **solve** conduction eq. using $\nabla \cdot Q_r = 0, T_N, \{\rho, k, C_p\}_{1,2}$, and $\{h_c, T_{amb}, T_{tool}\}$
return $T(t)$

The results obtained by the RTE-conduction for near-normal and grazing laser incidences are presented in Figs. 5a and 5b, respectively. Notably, a very good agreement with the experimental results of [6] can be observed during the heating and cooling phases. The results are in accordance with those obtained by the thermo-optical model using the RT approach as well. The temperature differences between the experimental and the numerical approaches proposed here at the most critical point (end of the heating phase) were 4.6°C and 5.8°C for the near-normal and grazing incidence scenarios, respectively. Nevertheless, these results fall within the uncertainty range of the experimental measurements, where the maximum uncertainties were estimated at ±10.5°C (±5.05% of $\bar{T}_{max}$=208.0°C) for the near-normal case and ±6.8°C (±3.25% of $\bar{T}_{max}$=211.5°C) for the grazing scenario. It is worth clarifying that these uncertainties were computed by repeating the experiment on five different samples in each case, and averaging the temperatures obtained in a

limited region of the heated area [6]. The main sources of these measurement uncertainties were: i) the thermal camera resolution, ii) tape surface heterogeneities, iii) within-batch tape variations, and iv) fluctuations linked to the setup conditions and operator manipulation. According to the camera manufacturer, the uncertainties resulting from the thermal measurements were estimated at ±2% and are comprised in the previously reported values.

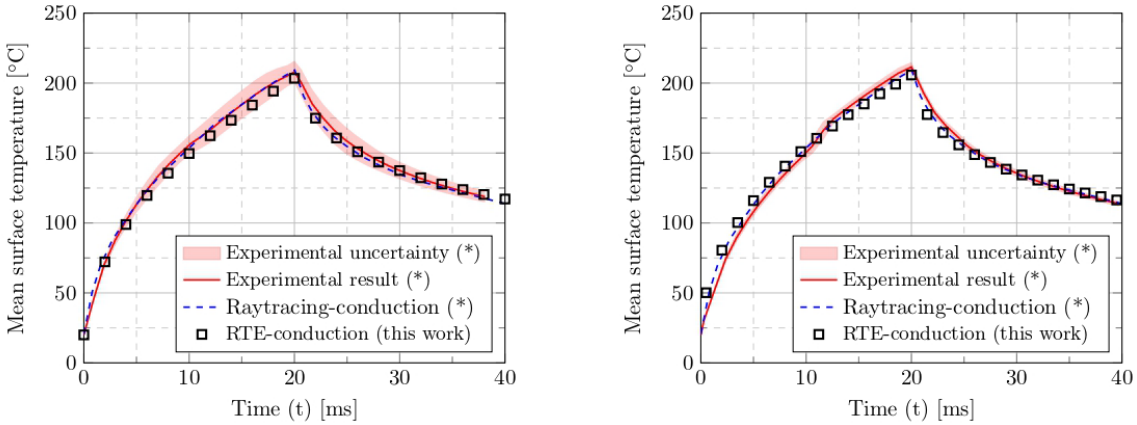

Figure 5: Transient temperature evolution of the composite surface obtained through the RTE-conduction approach. (*) Experimental and numerical research conducted by Le Reun et al [6].

RTE-Conduction on a 3D Case. To assess the feasibility of addressing complex geometries with the RTE-conductive approach, let us assume a 3D case where the fibers and the matrix domains are extruded in the z-axis direction by 100µm. The mesh used for the conductive heat transfer within the composite is obtained by extruding the elements of the 2D mesh of Fig. 1b, resulting in 3.451.200 tetrahedral elements. To solve the RTE, a reduced domain was employed accounting for the first's four fiber layers (see Fig. 6a) prioritizing an accurate solution in such a region and considering the large memory requirements of the RTE solver in 3D cases [10]. Then, the RTE mesh is conformed by a total of 3.879.000 tetrahedral elements (see Fig. 6b). A linear interpolation is performed to transfer the results obtained in the reduced 3D RTE domain to the full 3D conductive one. The RTE boundary conditions are those of the near-normal case depicted on Table 1, and the boundary conditions for the conductive heat transfer are identically to the ones presented in the previous subsection. The RTE solution took in total 24 minutes on 160 cores with $N_d = 160$ directions by using the GMRES solver, and it is presented in Fig. 6c. The results obtained at four different times by performing the RTE-conduction coupling is presented in Fig. 7, taking an additionally of 18 minutes. During the heating phase, which is the most critical one, the temperature delta at the top surface of the composite is of roughly 6°C. This is strictly linked to the laser orientation and microfibers arrangement, emphasizing the necessity for accurately modeling the radiative heat source.

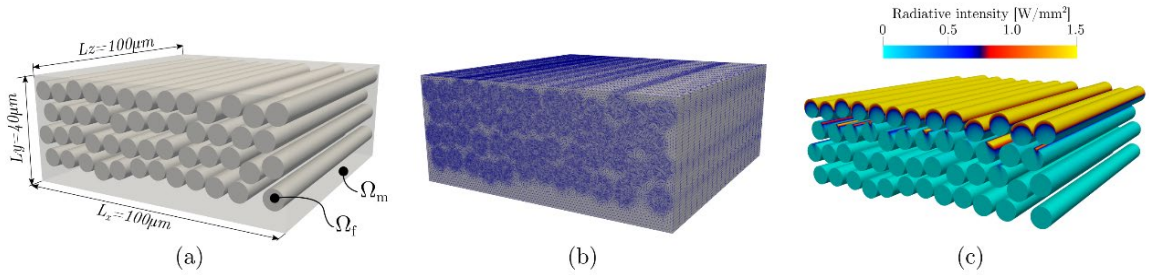

Figure 6: 3D radiative heat transfer on composite micro-structure: (a) reduced computational domain, (b) unstructured mesh of tetrahedral elements, and (c) the resulting radiative density field.

In contrast, during the cooling phase, such delta temperature diminishes to less than 1°C. It can further be noticed from Fig. 7 that, as expected, the heat flux is much higher within the fibers than within the matrix. This is mainly due to the higher fiber thermal conductivity, which is of roughly one order of magnitude superior compared to the one of the matrix.

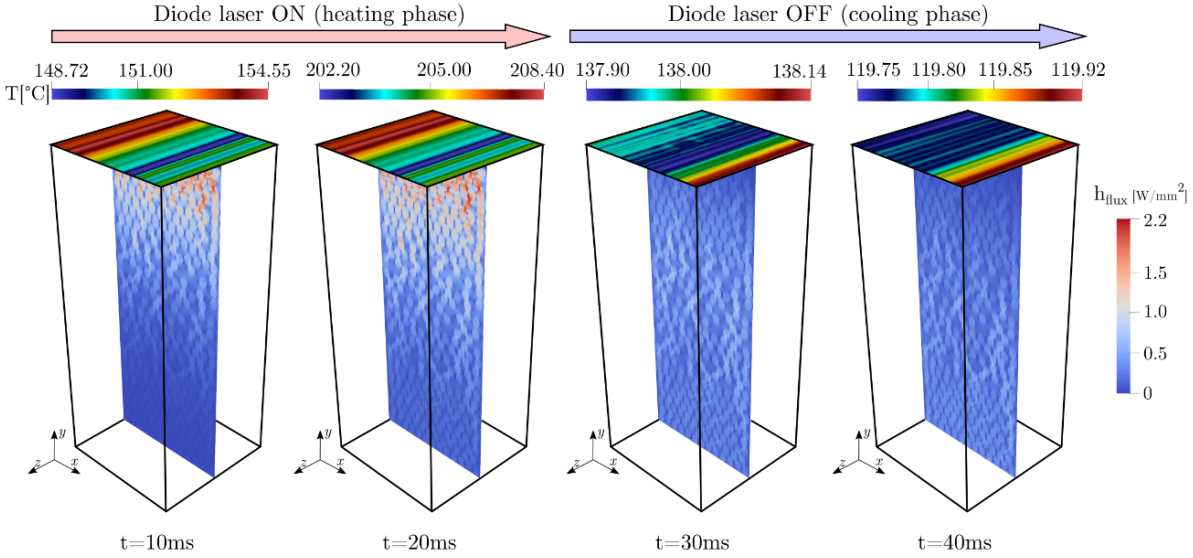

Figure 7: Result of the 3D RTE-conductive coupling 3D on the composite micro-structure showcasing the temperature field at the irradiated surface, and the heat flux within the composite.

Conclusions and future work

A numerical methodology based on a one-way coupling of the finite element radiative-conductive heat transfer equations specifically conceived for accurate modeling of the temperature evolution within a composite micro-structure facing typical AFP process conditions with varying laser beam incidence and intensity was presented in this work. The scheme allows addressing materials with high contrast thermal properties encountered within the composite material for the matrix and fibers such as the absorption coefficient and the thermal conductivity. A parametric study allowed the proper identification of the absorption coefficient of the carbon fibers, a critical parameter to accurately compute the radiative heat source term, and the results showed good agreement on a 2D scenario when compared to a ray-tracing approach reported in the literature. Furthermore, the RTE-conductive coupling was successfully solved on an artificial generated composite micro-structure resulting in 5-6°C maximal process temperature difference with respect to experimental and numerical results. These results propose a solid base for the accurate modeling of the laser-matter interaction on complex micro-structure geometries, and future works concern proper

heating law identifications in the AFP context featuring varying fiber orientations and volume fractions. Furthermore, internal reflections effects will be also considered.

References

[1] A. Levy, J. Tierney, D. Heider, J. Gillespie, P. Lefebure, D. Lang, Modeling of inter-layer thermal contact resistance during thermoplastic tape placement, in: International SAMPE Technical Conference, Baltimore, MA, USA, 2012.

[2] M. J. Donough, N. A. St John, A. W. Philips, B. G. Prusty, et al., Process modelling of in-situ consolidated thermoplastic composite by automated fibre placement–a review, Composites Part A: Applied Science and Manufacturing (2022) 107179. https://doi.org/10.1016/j.compositesa.2022.107179

[3] P. Hörmann, D. Stelzl, R. Lichtinger, S. Van Nieuwenhove, G. M. Carro, K. Drechsler, On the numerical prediction of radiative heat transfer for thermoset automated fiber placement, Composites Part A: Applied Science and Manufacturing 67 (2014) 282–288. https://doi.org/10.1016/j.compositesa.2014.08.019

[4] V. Le Louët, Etude du comportement thermique de bandes composites pré-imprégnées au cours du procédé de fabrication AFP avec chauffage laser, Ph.D. thesis, Université de Nantes (2018).

[5] O. Baho, G. Ausias, Y. Grohens, J. Férec, Simulation of laser heating distribution for a thermoplastic composite: Effects of AFP head parameters, The International Journal of Advanced Manufacturing Technology 110 (2020) 2105–2117. https://doi.org/10.1007/s00170-020-05876-9

[6] A. Le Reun, V. Le Louët, V. Sobotka, S. Le Corre, Numerical simulation at the micro-scale for the heat transfer modeling in the thermoplastic composites laser-assisted AFP process, Composites Part A: Applied Science and Manufacturing 28 (2023) 1897–1906. https://doi.org/10.1016/j.compositesa.2024.108010

[7] V. Le Louët, A. Le Reun, V. Sobotka, S. Le Corre, Experimental measurement of CF/PEKK tapes heating behavior in the laser assisted automated fiber placement process, in: 26th International ESAFORM Conference, 28 (2023) 1897–1906. https://doi.org/10.21741/9781644902479-205

[8] C. Stokes-Griffin, P. Compston, A combined optical-thermal model for near-infrared laser heating of thermoplastic composites in an automated tape placement process, Composites Part A: Applied Science and Manufacturing 75 (2015) 104–115. https://doi.org/10.1016/j.compositesa.2014.08.006

[9] F. Hecht, New development in FreeFEM++, Journal of numerical mathematics 20 (3-4) (2012) 251–266. https://doi.org/10.1515/jnum-2012-0013

[10] M. A. Badri, Efficient finite element strategies for solving the radiative transfer equation, Ph.D. thesis, Université de Nantes (2018). https://doi.org/10.1016/j.jqsrt.2018.03.024

[11] M. Badri, P. Jolivet, B. Rousseau, S. Le Corre, H. Digonnet, Y. Favennec, Vectorial finite elements for solving the radiative transfer equation, Journal of Quantitative Spectroscopy and Radiative Transfer 212 (2018) 59–74. https://doi.org/10.1016/j.jqsrt.2018.03.024

[12] M. Avila, R. Codina, J. Principe, Spatial approximation of the radiation transport equation using a subgrid-scale finite element method, Computer Methods in Applied Mechanics and Engineering 200 (5-8) (2011) 425–438. https://doi.org/10.1016/j.cma.2010.11.003